Available online at www.sciencedirect.com

ScienceDirect

Procedia CIRP 33 (2015) 562 – 567

www.elsevier.com/locate/procedia

9th CIRP Conference on Intelligent Computation in Manufacturing Engineering - CIRP ICME '14

Optimization of friction stir welding of thermoplastics

A. Paoletti, F. Lambiase*, A. Di Ilio

Dept. of Industrial and Information Engineering and Economics, University of L'Aquila, Via Campo Di Pile, 67100 AQ, Italy

* Corresponding author. Tel.: +39 0862 434343; fax: +39 0862 434303. *E-mail address:* francesco.lambiase@univaq.it

Abstract

Friction stir spot welding (FSSW) of thermoplastic materials has been recently developed. Early investigations have proved that such joining technology allows achieving high quality joints over conventional welding processes. In this paper, Friction spot stir welding is applied to Polycarbonate sheets of 3 mm thickness. A prototypal setup is developed to monitor the evolution of main forces and tool temperature during the joining phases. The influence of the main process parameters on the joints strength has been assessed by mean of single lap shear test on single joint. The joints quality has been also assessed by means of optical microscopy analysis. Finally an Artificial Neural Network has been developed in order to predict the mechanical behavior of the welded joints.

Selection and peer-review under responsibility of the International Scientific Committee of "9th CIRP ICME Conference"

Keywords: Joining, Polymers, Modelling, Polymer, Friction Stir Welding

1. Introduction

Thermoplastic materials are widely employed in different industrial and engineering applications in order to reduce product weight, thermal conductivity and to enhance toughness and stress-to-weight ratio. Joining methods for similar and dissimilar polymer structures are used in the automotive industry [1, 2]. Polymer welding methods are typically divided into three categories: techniques based on heat conduction, processes based on heat radiation and friction welding methods.

In the Friction Stir Welding (FSW) process, a non-consumable, rotating tool with a specific geometry is plunged into and traversed through the material. The two key components of the tool are the shoulder and the pin (probe). During welding, the pin travels in the material, while the shoulder rubs along the surface. Heat is generated by the tool shoulder rubbing on the surface and by the pin mixing the material below the shoulder. This mixing action permits the material to be transferred across the joint line, allowing a weld to be made without any melting of the material. Other than the linear process described above, another major variation of the process is Friction Stir Spot Welding (FSSW). The FSSW process involves only the plunge and retraction of the FSW tool, thus eliminating the traverse part of the process. The FSSW process mimics the Resistance Spot Welding (RSW) process and can be used in place of RSW, riveting, clinching or any other single point joining processes in many applications. It was claimed that for spot FSW the use of energy significantly decreased and the investment cost was about 40% lower due to its minimal equipment requirement. In addition, spot FSW is an environmentally friendly spot welding method due to the absence of fumes or sparks [3].

Friction stir spot welding was initially developed in the automotive industry to replace resistance spot welding for aluminum sheets [4-6]. Being a solid-state process, diffusion plays a central role during joining and metals are particularly suitable for this technique. Moreover, the high thermal conductivity of metals enhances material softening near the pin. For this reason, the process has been successfully applied to aluminum, magnesium and steel sheets, but there are very few publications on polymer friction stir spot welding applications [7, 8]. Recently, some researchers have studied the application of FSSW to thermoplastics but obtaining good joints is a very hard task. In fact, thermoplastic materials are poor thermal conductors and diffusion is not an efficient mechanism because of their macromolecular structure.

Selection and peer-review under responsibility of the International Scientific Committee of "9th CIRP ICME Conference"
doi:10.1016/j.procir.2015.06.078

The effect of tool geometry on plastic flow and mixing of materials during friction stir spot welding is investigated numerically using the particle method [9]. Tool geometry has a significant influence on the material mixing and hence eventually influences the static strength of resultant spot welds. Moreover, tool material properties such as strength, fracture toughness, hardness, thermal conductivity and thermal expansion coefficient affect the weld quality, tool wear and performance [10, 11].

In the field of plastic materials, FSSW has been successfully applied to high density polyethylene (HDPE), polypropylene (PP), polymethylmethacrylate (PMMA) and acrilonitrile butadiene styrene (ABS) sheets [12-14]. In a wide range of lighting applications including automotive lighting, there is a need to join PMMA to ABS to reduce costs and increase performance of lamps. Although PMMA and ABS are dissimilar materials, they are compatible with each other and are frequently blended or welded together [15]. Welding of PMMA to ABS by friction stir spot welding is feasible and process parameters have a significant effect on weld strength. The lap-shear strength of welded PMMA/ABS specimens was investigated as the mechanical property of the joints. Results indicate that variable parameters of process including tool rotational speed, tool plunge rate and dwell time, have dramatical influence on the weld strength [16]. The effects of tool penetration depth and dwell time on joint strength of polypropylene using a conventional tool was also investigated; increasing the dwell time causes a significant improvement on tensile shear strength, however there is an optimal point for tool penetration [17]. An improved tool in which the pin and shoulder could rotate independently of each other was used for of FSSW of PMMA plates. The results showed that the weld strength is comparable to other available welding techniques, while the joining times are equal or shorter [18].

This paper introduced a preliminary work aimed at optimizing the operative conditions in friction spot stir welding process of thermoplastic materials. To this end, a prototypal setup has been developed to monitor the evolution of plunging force, torque and tool temperature during the joining phases of Polycarbonate (PC) friction spot stir welding. A campaign of experimental tests involving the variation of the main process parameters was conducted and the collected data were used to develop an Artificial Neural Network, which is aimed at predicting the maximum plunging force, maximum torque and temperature as well as the shear strength of friction spot stir welded connections.

2. Experimental setup

The experimental set up consists of a drilling press equipped with a servo-system, an asynchronous motor driven by an inverter, a piezoelectric dynamometer, and an infrared pyrometer, as shown in Figure 1.

The servo-system has allowed to regulate the axial tool plunge rate, while the inverter has been used to adjust the revolution speed of the spindle motor. Both systems have been controlled by a computer. Plunging force and torque signals have been detected by means of a piezo-electric dynamometer, filtered by low-pass filters and acquired by data acquisition card.

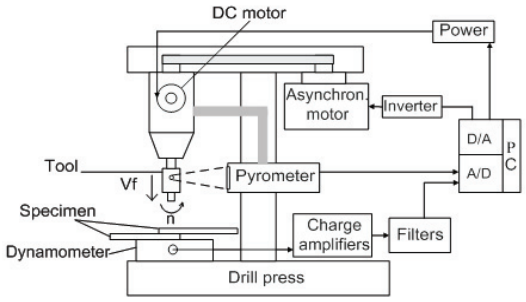

Fig. 1. Experimental apparatus.

Contactless temperature measurements have been carried out employing a radiation sensor type 1060-2 in connection with Thermophil INFRA type 4472 thermometer. The sensor detects the IR radiation heat emitted by the tool and converts it into an electrical signal which is amplified, processed and then acquired by the computer. Type T1060-2 sensor acquires the radiation on a measuring field of 3 mm diameter from a distance of 100 mm, which can be adjusted by means of a focusing device. Temperature measurements has been taken at a fixed distance from the tool-workpiece interface.

3. Experimental procedure

Polycarbonate sheets having 3 mm thickness, 20 mm width and 90 mm length have been cut from commercial plates. Polycarbonate is an amorphous thermoplastic polymer having a tensile strength of about 58÷62 MPa, a glass transition temperature of about 147° C and a melting temperature of about 155 °C.

The specimens have been overlapped by 30 mm in length. Figure 2 shows the polycarbonate specimens in lap position.

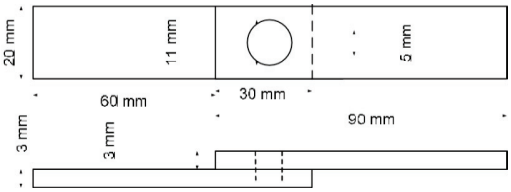

Fig. 2. Typical configuration of the lap-shear test specimen.

A view of the tool, which is used in this investigation, is shown in Figure 3.

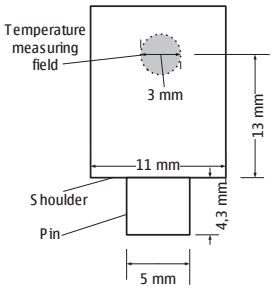

Fig. 3. Frontal view of the tool used for the tests.

The tool has a shoulder diameter of 11 mm, a pin diameter of 5 mm, and a pin length of 4,3 mm, and is made from a low carbon steel. Tool temperature has been measured at 13 mm distance from the shoulder. The FSSW process consists of three phases; plunging, stirring and retracting. The process starts with spinning the tool with a high rotational speed (n). Subsequently, the tool is approached in the weld spot until the pin of the tool touches the surface of the upper workpiece (Figure 4).

At this moment, the feed is stopped and the rotation produces a material heating for a period called preheating time (Pt). Then the tool is plunged into the material adopting a tool plunge rate (vf) as far as the shoulder of the tool comes in contact with the upper surface of the workpiece. The plunge movement of the tool causes material expulsion. When the tool reaches the predetermined depth, the plunge motion ends and the stirring phase starts. In this phase, the tool rotates inside the workpiece without plunging for a time called the dwell time (Dt). Frictional heat is generated in the plunging and the stirring phase and, thus, the material adjacent to the tool is heated and softened. The softened upper and lower workpiece materials mix together in the stirring phase. When the predetermined dwell time is reached, rotation of the tool is immediately stopped. The tool remains in the workpiece for a waiting time (Wt) after the end of the stirring phase. The shoulder of the tool creates a pressure on the softened material, under which a solid-state joint is formed. After a predetermined time is obtained, the process stops and the tool is retracted from the workpiece. The resulting weld has a characteristic keyhole in the middle of the joint.

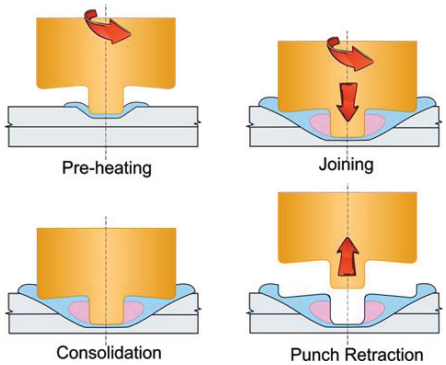

Fig. 4. Typical phases of friction stir spot welding process: pre-heating, joining, consolidation and tool retraction.

A two-level full factorial design of experiments has been adopted selecting five factors as follows: tool plunge rate, tool rotation speed, pre-heating time, dwell time and waiting time. In order to detect curvature in the fitted data, centre point has been added to the factorial design. In the factorial points, a single experimental run has been carried out, while in centre point four replicates have been conducted. The welding parameters and the values employed in this study are given in Table 1.

Table 1: Welding parameters.

Symbol	Welding parameter	Low level [-1]	Centre point [0]	High level [+1]
v_f	Tool plunge rate [mm/min]	8	27	46
n	Tool rotation speed [rpm]	1500	3450	5400
P_t	Pre-heating time [s]	0	10	20
D_t	Dwell time [s]	0	10	20
W_t	Waiting time [s]	0	10	20

4. Analysis of preliminary results

Figures 5 shows the evolution of plunging force (Figure 5a), the torque (Figure 5b) and the tool temperature (Figure 5c) during the joining phases. Plunging force reaches a maximum value (F_{max}) just after the contact with the surface of the upper sheet (point A). Then the force decreases and remains constant until the shoulder of the tool comes in contact with the surface of the upper workpiece (point D of the graph 5). This force has been called steady-state force (Fss) and the value is determined at the point in which the pin of the tool is in contact with the surface of the lower workpiece (point B). After the contact of the shoulder with the surface of the upper workpiece, the tool move forward for about further 0.6 mm, so as to apply a clamping force,Fc, to the joint that is being realized (point Y). The control of Fc is done on the axial displacement, for which its value depends on the value set by the welding parameters for the single test. By analyzing the trend of the torque, the value C1 is measured at the point in which the pin of the tool is in contact with the surface of the lower workpiece. Cmax represents the maximum value of the torque, while Cc is the clamping torque (point L). The tool temperature measured by the infrared pyrometer, shows a nonlinear increase as a function of tool axial displacement. The value T2 is obtained when the shoulder of the tool is in contact with the surface of the upper workpiece (point U), while the maximum value of the temperature, Tmax, is reached when the tool is applying the clamping force to the welded joint. The weld quality of a spot weld is usually defined by its strength. In Figure 8 a typical trend of tensile force as a function of displacement, during a single lap shear test on single joint, is reported. The welded joint is characterized by a linear-elastic behavior as far as the breaking force, Fr, is reached. The breaking force of the welded joint can be indicated as the lap shear strength. The value dr represents the displacement reached in correspondence of the breaking force.

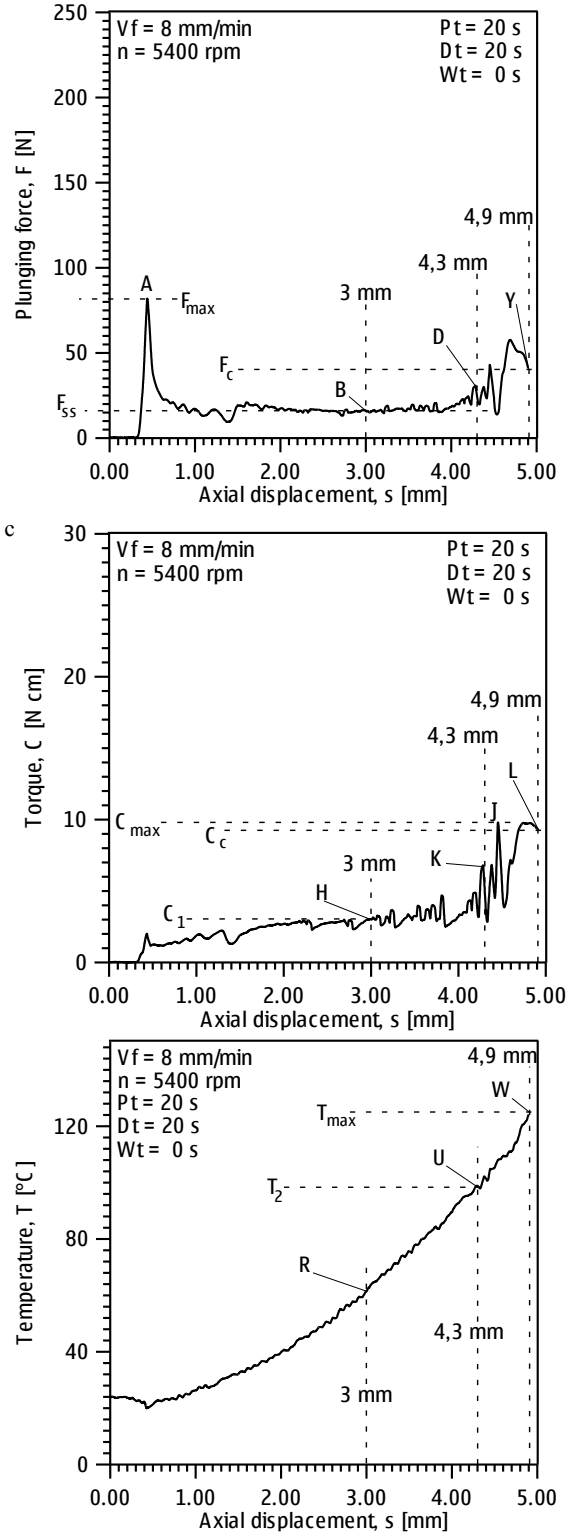

Fig. 5. Typical trend of plunging force torque and tool temperature as a function of tool axial displacement.

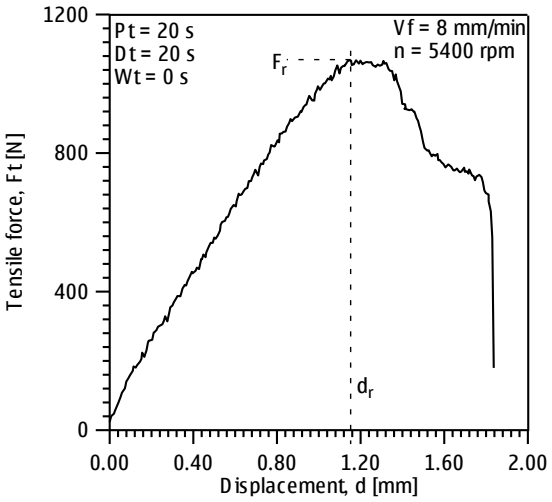

Fig. 6. Typical trend of tensile force as a function of displacement.

As mentioned above, according to preliminary test results, the mechanical strength of friction stir welding spot connections is mainly influenced by the plunge rate, the rotational speed and the waiting time. Particularly, the maximum lap shear strength was obtained for the welded joint obtained by selecting low levels of tool plunge rate and tool rotational speed and high levels of pre-heating, dwell and waiting times. On the other hand, high level of tool plunge rate and low levels of tool rotational speed, pre-heating, dwell and waiting times generated the joint with the lowest mechanical behaviors. In this experimental conditions the lap shear strength is equal to 224 N. The cross sections of the joints with the highest and lowest mechanical strength are reported in Figure 7 a and b, respectively. As can be observed, the joint with the highest strength exhibits a large welded area, whose width r = 1.5 mm, while the welded area in the joint depicted in Figure 7 b is almost imperceptible (width r = 0.1mm). The area of the welded zone in the first sample is given by $((R+r)^2-R^2) \times \pi = (2.5+1.5)^2-2.5^2) \times \pi = 24.3$ mm^2. Thus considering the maximum strength of the joint F_{max} = 1470 N, it results a tensile stress of about 60 MPa. The tensile stress of the joint is close to the one of the material, which is about 58÷62 MPa. For all the welds, it was observed that a depression has been left by the tool shoulder and a keyhole formed at the center of the welds, which are the typical characteristics of the sample made by FSSW. A portion of workpiece material has been lost in the welded cordon, because polycarbonate particles are rotated by the tool and ejected from the weld zone under the effect of the inertia forces. It is also possible to observe the presence of air blisters on the welded joints. Blister formation is produced by material cooling process and it is more evident when higher temperature values have been reached (Figure 7a). At high rotational speeds, a higher amount of heat is transferred to the material due to friction. However, if the rotational speed is too high, the material gets parted by the pin and a poor joining has been obtained.

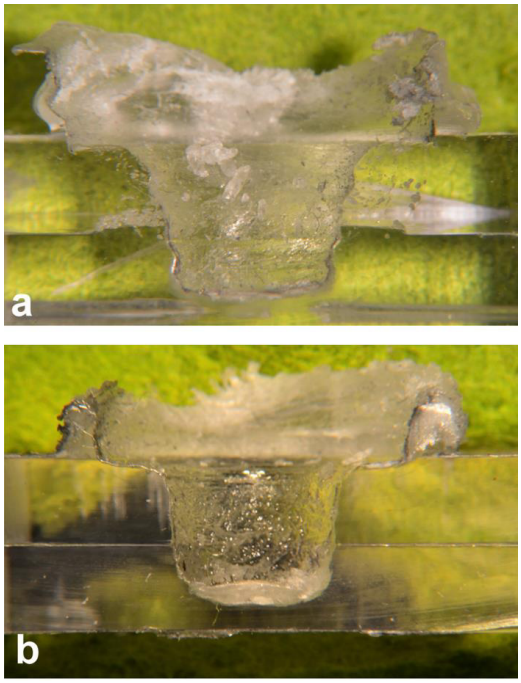

Fig. 7. Cross sections of joints produced under different processing conditions leading to: (a) highest strength and (b) lowest strength.

Figure 8 depicts the flow chart of the optimization system development in this work. As can be observed, after an initial guess of the process parameters, the procedure compares the maximum force F_{max} and torque C_{max} (predicted by the ANN model) with the machine limits. After the compatibility check, the ANN model predicts the joint strength F_r and proceeds with the optimization

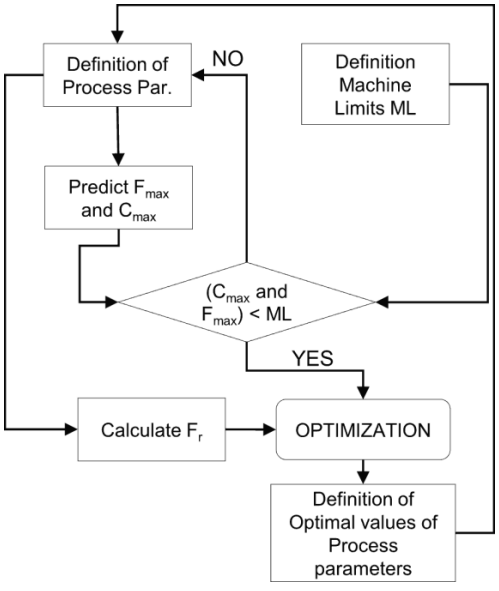

Fig. 8. Flow chart of the optimization algorithm

4.1. Prediction of mechanical behaviors of welded joints by Neural Networks

The optimization of the process parameters aimed at maximizing the mechanical strength of friction spot stir welded joints requires the development of a model able to predict the mechanical strength of a joint according to the process parameters. In addition, to check the feasibility of the process on a given drilling/milling machine, it is also important to verify that the involved process conditions do not require a plunging force and a torque exceeding the machine limits.

To this end, an Artificial Neural Network (ANN) was developed. Artificial Neural Networks are soft computing and modelling techniques that are able to learn nonlinear relationships between almost any number of inputs and any number of outputs. Successful employment of such modelling/mapping techniques can be found in several fields of engineering, sciences, medicine etc. Recent development of ANN models in the field of process design and optimization concern automatic systems for roll pass design [19], laser hardening optimization [20] and design and optimization of tools geometry of clinching tools [21].

In the present investigation, an ANN composed by three layers was developed. Preliminary tests were conducted in order to determine the optimal ANN configuration and specifically the number of neurons in the hidden layer. Figure 8 shows the trend of RMSE varying the number of neurons (N) in the hidden layer. The ANN model with 11 neurons in the hidden layer ensures a good fitting with an RMSE of 0.07 for the testing set and a correlation coefficient $R^2 = 0.95$. According to the achieved results, the number of neurons which minimises the RMSE is 11, as shown in figure 9. The ANN was trained by a feed forward back propagation algorithm within Matlab Framework. The training dataset was based on a full factorial experimental plan 3^3. Intermediate values between experimental levels were also used to enlarge the training set. Actually, according to a preliminary analysis of sensitivity, the main operational conditions influencing the mechanical strength of spot connections produced by friction stir welding were: the plunge rate, the rotational speed and the dwell time.

The network was composed by an input layer of 3 neurons (n, vf and Dt), an hidden layer composed by 11 neurons and an output layer composed by 9 neurons comprising the characteristics values of the plunging force (Fss, Fc, Fmax) torque (C1, Cc, Cmax) and temperature (T2 and Tmax) measured during the joining operations and the shear resistance of the joint (Fr).

Figure 10 shows the fitting between the Neural Network model and the experimental data. As can be noted, the model correlates well with experimental measurements as also confirmed by the low values of the Mean Absolute Errors (MAE) which is ~2% for F_{max}, ~3% for C_{max} and ~5% for F_r. According to the achieved results, the developed ANN model allows to accurately predict the main operative conditions (force and torque) arising during the friction spot stir welding process as well as the mechanical strength of the produced joints.

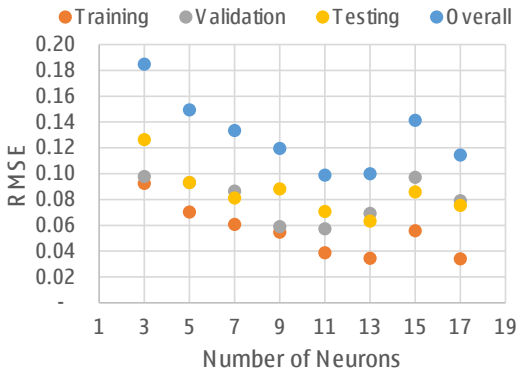

Fig. 9. Trend of RMSE by varying N in the hidden layer of the network.

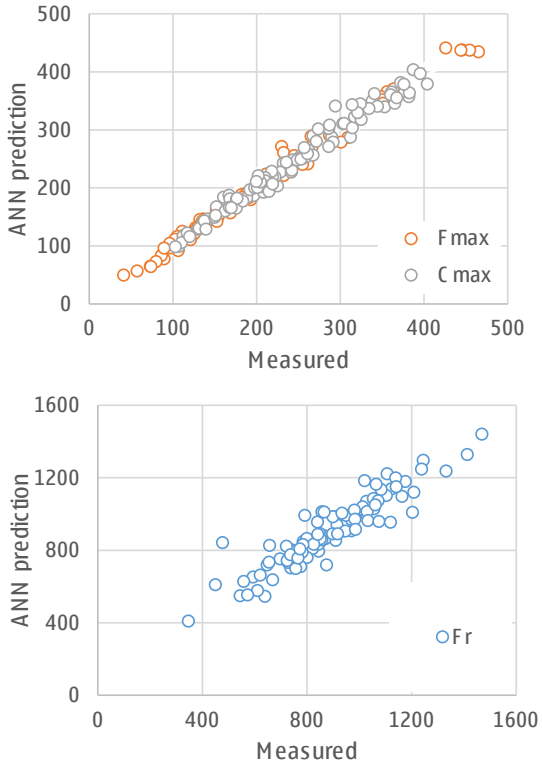

Fig. 10. Comparison between experimental data and Neural Network predictions.

5. Conclusions

Friction stir spot welding of thermoplastic materials is a promising technique because of some advantages over other joining technologies, as the low cost of machine and tooling cost. In such conditions very high strengths may be obtained, close to the strength of the base material.

The effect of friction stir spot welding parameters on the maximum plunging force, maximum torque and joint strength of polycarbonate sheet welds has been modelled by means of Artificial Neural Network. The accuracy of the ANN model predictions has been evaluated by considering different indicators including the mean square error, maximum error and correlation coefficient R^2. From this preliminary work it emerged that the developed model can be successfully adopted as a "process knowledge block" to be integrated with an optimization procedure for automatic process design of friction spot stir welding.

References

[1] M. K. Bilici, Application of Taguchi approach to optimize friction stir spot welding parameters of polypropylene, Materials and Design, 35: 113–119, 2012.
[2] E. Azarsa, A. Mostafapour, On the feasibility of producing polymer–metal composites via novel variant of friction stir processing Journal of Manufacturing Processes, 15, (4): 682-688, 2013.
[3] Y.F. Sun, J.M. Shen, Y. Morisada, H. Fujii, Spot friction stir welding of low carbon steel plates preheated by high frequency induction, Materials and Design, 54: 450–457, 2014.
[4] R. Hancock, Friction welding of aluminium cuts energy cost by 99%, Welding Journal, 83: 40, 2004.
[5] D.A. Wanga, S.C. Leeb, Microstructures and failure mechanisms of friction stir spot welds of aluminum 6061-T6 sheets, Journal of Material Processing Technology, 7: 186:291, 2007.
[6] A. Gerlich, P. Su, T. H. North, Tool penetration during friction stir spot welding of Al and Mg alloys, Journal of Materials Science, 40: 6473–6481, 2005.
[7] B.T. Gibsona, D.H. Lammleinb, T.J. Praterc, W.R. Longhurstd, C.D. Coxa, M.C. Balluna, K.J. Dharmaraja, G.E. Cooka, A.M. Strauss, Friction stir welding: process, automation, and control, Journal of Manufacturing Processes, 2013.
[8] L. Wan, Y. Huang, Z. Shixiong, J. Feng, Effect of self-support friction stir welding on microstructure and microhardness of 6082-T6 aluminum alloy joint, Materials and Design, 55: 197–203, 2014.
[9] S. Hirasawaa, H. Badarinarayanb, K. Okamotoc, T. Tomimurad, T. Kawanami, Analysis of effect of tool geometry on plastic flow during friction stir spot welding using particle method, Journal of Materials Processing Technology, 210: 1455–1463, 2010.
[10] R. Rai, A. De, H.K. Bhadeshia, T. DebRoy, Review: friction stir welding tools, Science and Technology of Welding and Joining, 16 (4): 325-343, 2011.
[11] R. Nandan, T. DebRoy, H.K.D.H. Bhadeshia, Recent advances in friction-stir welding–Process, weldment structure and properties, Materials Science, 53, (6): 980-1023, 2008
[12] M.K. Bilici, A.İ. Yükler, M. Kurtulmuş, The optimization of welding parameters for friction stir spot welding of high density polyethylene sheets, Materials & Design, 32, (7): 4074-4079, 2011.
[13] M. K. Bilici, A. I. Yukler, Effects of welding parameters on friction stir spot welding of high density polyethylene sheets Materials & Design, 33: 545-550, 2012.
[14] A. Bagheri, T. Azdast, A. Doniavi, An experimental study on mechanical properties of friction stir welded ABS sheets, Materials & Design, 43: 402-409, 2013.
[15] A. Mokhtarzadeh, C.Y. Wu, A. Benatar, Comparation of hot plate and vibration welding of PMMA to ABS, ANTEC, 856–861, 2000.
[16] S.H. Dashatan, T. Azdast, S.R. Ahmadi, A. Bagheri, Friction stir spot welding of dissimilar polymethyl methacrylate and acrylonitrile butadiene styrene sheets, Materials and Design, 45: 135-141, 2013.
[17] A. Armagan, M. Senol, Friction stir spot welding of polypropylene. Journal of Reinforced Plastic Composites, 27: 2001–2004, 2008.
[18] P.H.F. Oliviera, S.T. Amancio-Filho, J.F. Dos Santos, J.E. Hage, Preliminary study on the feasibility of friction spot welding in PMMA, Material Letters, 64: 2098–2101, 2010.
[19] F. Lambiase, Optimization of shape rolling sequences by integrated artificial intelligent techniques, The International Journal of Advanced Manufacturing Technology, 68: 443-452, 2013.
[20] F. Lambiase, A. M. Di Ilio and A. Paoletti, Prediction of Laser Hardening by Means of Neural Network, *Procedia CIRP*, 12: 181-186, 2013.
[21] F. Lambiase and A. Di Ilio, Optimization of the Clinching Tools by Means of Integrated FE Modeling and Artificial Intelligence Techniques, Procedia CIRP, 12: 163-168, 2013.